Journal of Sound and Vibration (2002) **258**(4), 577–594
doi:10.1006/jsvi.2002.5175, available online at http://www.idealibrary.com on IDEAL®

INHOMOGENEOUS WAVES IN ANISOTROPIC POROUS LAYER OVERLYING SOLID BEDROCK

A. K. Vashishth and P. Khurana

Department of Mathematics, Kurukshetra University, Kurukshetra 136119*, India.*
E-mail: kuta@vidya.kuk.ernet.in

(*Received* 9 *January* 2001, *and in final form* 31 *January* 2002)

The problem of propagation of inhomogeneous waves in anisotropic porous layered medium is studied using transfer matrix. Firstly, transfer matrix for an anisotropic porous layer is derived. Biot's poro-elastic theory is incorporated to model the acoustics of anisotropic porous layer. The interface between porous layer and elastic half-space is considered as imperfect and modified boundary conditions are applied for this more realistic situation. The theory of transfer matrix is used to derive the analytical expression for the surface impedance. Numerical computation of results is done for different degrees of bonding in the low as well as high-frequency range. In the first case, which is relevant to geophysical studies, the surface impedance is predicted for low-frequency range and surface impedance for second model is computed in high-frequency range. It is observed that loose bondedness is accompanied by the loss of energy at the interface. The technique of transfer matrix is utilized to compute the surface impedance in both cases. The role of surface impedance in seismological studies and in the study of composites is discussed.

1. INTRODUCTION

Because of its practical importance in various fields such as earthquake engineering, soil dynamics, geophysics, etc., much attention is given to the wave propagation in fluid-saturated porous media. Biot [1, 2] developed the theory of plane wave propagation in saturated porous media in his two classic papers, which still dominates the field. Nagy *et al.* [3] studied the slow wave propagation in air-filled porous materials and natural rocks. Buckingham [4,5] studied the wave propagation in consolidated and non-consolidated marine sediments and established the expressions for wave speeds and attenuation.

Studies of propagation of elastic waves in layered porous media have long term of interest to researchers in the field of geophysics, acoustics and non-destructive evaluation. Plane wave propagation in layered porous media at normal as well as oblique incidence is studied by Allard *et al.* [6, 7]. Lauriks *et al.* [8] used the method of transfer matrix in the study of plane wave propagation in layered media. Adler [9] applied the matrix method to study acoustic waves in multilayers. Practically, saturated porous materials are anisotropic due to bedding, compaction and presence of aligned microcracks. Anisotropy may have significant effects on wave characteristics in layered media. Nayfeh [10, 11] studied the general problem of elastic wave propagation in multilayered anisotropic media using transfer matrix. Badiey *et al.* [12] applied propagator matrix method for plane wave reflection from inhomogeneous anisotropic poro-elastic seafloor. Potel and de Belleval [13] studied the propagation of waves in an anisotropic periodically multilayered medium. Rayleigh waves on the surface of transversely isotropic liquid-saturated porous layered

0022-460X/02/$35.00

medium was studied by Sharma *et al.* [14]. They found that existence and speed of Rayleigh waves is affected by transverse isotropy of considered medium. Schmitt [15] investigated the properties of the modes generated by multiple sources in a fluid-filled borehole embedded in foundations which include transversely isotropic poro-elastic layers.

Usually, perfect bondings, which ensure continuity of all field variables, between the layers are encountered. But in some elastodynamic problems, the bonding between layers may be imperfect which is a reasonable assumption for layered media including porous layers. The usual continuity conditions are inadequate to describe the wave interaction with such an imperfect interface. Vashishth *et al.* [16] presented modified boundary conditions at imperfect interface between elastic half-space and poro-elastic half-space.

The acoustical properties of fluid-saturated, homogeneous and isotropic porous materials are completely specified when characteristic impedance and wave number, or two independent properties derived from them, e.g. complex density and complex sound speed are known. Thus, it is of interest to be able to determine experimentally and analytically the wave number and the characteristic impedance of homogeneous isotropic porous media [17]. The study can also be useful in many types of sound absorbing materials, which include for example glass fiber, polymeric fibrous materials and various types of foams.

In this paper, reflection and transmission of waves in a layered media have been studied through a physical quantity named surface impedance. The transfer matrix for anisotropic poro-elastic solid layer has been obtained analytically. Two different models are considered for the study of surface impedance with the use of transfer matrix so obtained. The first one consists of anisotropic poro-elastic layer between fluid and elastic solid half-space and the second one has two anisotropic porous layers under the fluid half-space. To be more close to realistic situations, the boundary between porous layer and elastic substratum, in general, is being considered as imperfect boundary and boundary conditions have been modified appropriately. The closed-form expression of acoustic surface impedance, in compact and convenient form, is obtained in both cases. Thus the use of transfer matrix saves a lot of computational time and enhances the efficiency of computer codes for numerical computation as the matrix notation suggests a systematic computational procedure, which greatly facilitates the computation.

2. BASIC EQUATIONS

Following Biot [1], the equations of motion for a porous medium are

$$\begin{aligned} &\tau_{ij,j} = \rho\ddot{\boldsymbol{u}}_i + \rho_f \ddot{\boldsymbol{W}}_i \quad (i,j = 1,2,3), \\ &-(p_f)_{,i} = \rho_f u_i + c_i \rho_f W_i/\beta' + F b_i W_i, \end{aligned} \tag{1}$$

where τ_{ij} is the stress tensor, p_f is the pore fluid pressure, ρ_f and ρ are the mass densities of the fluid and the bulk porous material, respectively, and β' is the porosity of the layer. $\mathbf{W} = \beta'(\mathbf{U} - \mathbf{u})$ is the relative displacement of fluid with respect to the solid and $\mathbf{U}$ and $\mathbf{u}$ are the displacements of saturant fluid and solid part of the porous medium. Coefficients b_i's are the friction parameters. Biot [2] has derived these as

$$b_i = \xi/k_i, \tag{2}$$

where ξ and k_i are the viscosity and permeability of the pore fluid. For cylindrical pores, the permeability is given by

$$k_i = (8/\bar{a}^2)\delta_i, \tag{3}$$

where $\bar{a}$ is the pore size and δ_i is the shape factor and its value is one for circular cylindrical pores. Function $F(\kappa)$ is a frequency-dependant viscosity factor, defined by

$$F(\kappa) = \kappa T(\kappa)/4\{1 - 2T(\kappa)/(\mathrm{i}\kappa)\}, \tag{4}$$

in which

$$T(\kappa) = \{ber'(\kappa) + \mathrm{i}\, bei'(\kappa)\}\{ber(\kappa) + \mathrm{i}\, bei(\kappa)\},$$
$$\kappa = \bar{a}(\omega\rho_f/\xi)^{1/2}.$$

Here $ber(\kappa)$ and $bei(\kappa)$ are the real and imaginary parts of the Kelvin's function and primes denote their derivatives.

The constitutive equations for a transversely isotropic porous medium were given by Biot [18] and these are

$$\begin{aligned}
\tau_{xx} &= 2B_1 e_{xx} + B_2(e_{xx} + e_{yy}) + B_3 e_{zz} + B_6\zeta,\\
\tau_{yy} &= 2B_1 e_{yy} + B_2(e_{xx} + e_{yy}) + B_3 e_{zz} + B_6\zeta,\\
\tau_{zz} &= B_4 e_{zz} + B_3(e_{xx} + e_{yy}) + B_7\zeta,\\
\tau_{yz} &= 2B_5 e_{yz}, \qquad \tau_{zx} = 2B_5 e_{zx}, \qquad \tau_{xy} = 2B_1 e_{xy},\\
p_f &= B_6(e_{xx} + e_{yy}) + B_7 e_{zz} + B_8\zeta,
\end{aligned} \tag{5}$$

where e_{ij} are the strain components of solid matrix; τ_{ij} are the total stress components of bulk material; and ζ is the increament of fluid content per unit volume which is defined by $\zeta = \mathrm{div}[\beta'(\mathbf{u} - \mathbf{U})]$. $B_1,\ B_2, \ldots, B_8$ are material coefficients. These are evaluated by applying the method developed by Hashin and Rosen [19] and by Christensen [20] for evaluating the material coefficients of composite materials. The equations which relate the coefficients $B_1, B_2, \ldots, B_8$ to the bulk modulus (K_s), shear modulus (μ_s), Young's modulus (E_s) and the Poisson ratio (v_s) of the solid grain and the bulk modulus (K_f) of the pore fluid, and to the porosity (β') are

$$\begin{aligned}
B_1 &= \mu_{12}, \qquad B_2 = K_{12} - \mu_{12},\\
B_3 &= 2v_{31}K_{12}, \qquad B_4 = E_{33} + 4v_{31}^2 K_{12},\\
B_5 &= \frac{1}{\mu_{13}},\\
B_6 &= -\frac{K_f(K_s + 4\mu_s/3)}{K_f + \mu_s + \beta'(K_s + \mu_s/3 - K_f)},\\
B_7 &= -K_f\left[1 + (1 - \beta')\frac{2v_s(K_s + \mu_s/3) - K_f}{K_f + \mu_s + \beta'(K_s + \mu_s/3 - K_f)}\right],\\
B_8 &= \frac{K_f[(K_s + \mu_s/3)\beta' + \mu_s]}{K_f + \mu_s + \beta'(K_s + \mu_s/3 - K_f)},
\end{aligned}$$

where

$$E_{33} = (1 - \beta')E_s + \frac{4\beta'(1 - \beta')(1/2 - 2v_s)^2}{(1 - \beta')/K_f + \beta'/(K_s + \mu_s/3) + 1/\mu_s},$$
$$v_{31} = (1 - \beta')v_s + \beta'/2 + \frac{\beta'(1 - \beta')(1/2 - v_s)[1/(K_s + \mu_s/3) - 1/K_f]}{(1 - \beta')/K_f + \beta/(K_s + \mu_s/3) + 1/\mu_s},$$

$$K_{12} = K_s + \mu_s/3 + \frac{\beta'}{1/(K_f - K_s - \mu_s/3) + (1-\beta')/(K_s + 4\mu_s/3)},$$
$$\mu_{13} = (1-\beta')/[(1+\beta')\mu_s],$$

μ_{12} is determined from the equation

$$A(\mu_{12}/\mu_s)^2 + 2B(\mu_{12}/\mu_s) + C = 0,$$

where

$$A = -3\beta'(1-\beta')^2 - (\eta_s + \beta'^3)(1+\beta'\eta_s),$$
$$B = 3\beta'(1-\beta')^2 + (1-\beta')(\eta_s - 1 + 2\beta'^3)/2 - \beta'/2(\eta_s+1)(1-\beta'^3),$$
$$C = -3\beta'(1-\beta')^2 + (1-\beta')(1-\beta'^3).$$

For two-dimensional wave motion in xz-plane, we can assume the plane harmonic solutions of equation (1) of the form

$$\begin{aligned} u_x &= a_1 \exp[\mathrm{i}\omega(t - x/c - qz)], \\ u_z &= a_3 \exp[\mathrm{i}\omega(t - x/c - qz)], \\ U_x &= b_1 \exp[\mathrm{i}\omega(t - x/c - qz)], \\ U_z &= b_3 \exp[\mathrm{i}\omega(t - x/c - qz)], \end{aligned} \tag{6}$$

where a_1, a_3, b_1 and b_3 are the wave amplitudes and c is the phase velocity.

Substitution of these solutions into equation (1) gives a set of four simultaneous equations in four unknowns a_1, a_3, b_1 and b_3. The existence of their non-trivial solution leads to a cubic equation in q^2 and is of the form

$$T_0 q^{6+} T_1 q^{4+} T_2 q^{2+} T_3 = 0, \tag{7}$$

where

$$\begin{aligned}
T_0 &= c_{11}B_5(B_7^2 - B_4B_8), \qquad T_1 = T_{11} + T_{12}/c^2, \\
T_2 &= T_{21} + T_{22}/c^2 + T_{23}/c^4, \qquad T_3 = T_{31} + T_{32}/c^2 + T_{33}/c^4 + T_{34}/c^6, \\
T_{11} &= c_{11}(B_4B_8 - B_7^2)\rho + c_{11}\rho B_5B_8 + 2c_{11}\rho_f B_5B_7 + c_{11}c_{33}B_4B_5 + \rho_f^2(B_7^2 - B_4B_8), \\
T_{12} &= c_{11}(2B_1 + B_2)(B_7^2 - B_4B_8) - c_{33}B_4B_5B_8 + c_{33}B_5B_7^2 + c_{11}(B_3^2B_8 + 2B_3B_5B_8) \\
&\quad - c_{11}B_6(2B_3B_7 + 2B_5B_7 - B_4B_6), \\
T_{21} &= -c_{11}\rho^2B_8 - 2c_{11}\rho\rho_f B_7 - c_{11}c_{33}\rho(B_4 + B_5) + c_{11}\rho_f^2B_5 + c_{33}\rho_f^2B_4 + \rho\rho_f^2B_8 + 2B_7\rho_f^3, \\
T_{22} &= \rho(c_{11}B_5B_8 + c_{33}B_4B_8) + \rho c_{11}(2B_1 + B_2)B_8 + 2c_{11}\rho_f B_7(2B_1 + B_2) - c_{33}\rho B_7^2 \\
&\quad + c_{11}c_{33}B_4(2B_1 + B_2) + c_{33}\rho B_5B_8 - 4\rho_f^2B_5B_8 - 2\rho_f(B_3 + B_5)(c_{11}B_6 + c_{33}B_7) \\
&\quad - 2\rho_f^2B_3B_8 - c_{11}c_{33}(B_3^2 - 2B_3B_5) + 2c_{33}\rho_f B_4B_6 + 2\rho_6^2B_6B_7 - c_{11}B_6^2\rho, \\
T_{23} &= c_{33}B_7^2(2B_1 + B_2) - (c_{11}B_5 + c_{33}B_4)\{(2B_1 + B_2)B_8 - B_6^2\} + c_{33}(B_3 + B_5)\{B_3B_8 - 2B_7B_6\}, \\
T_{31} &= \rho^2c_{11}c_{33} - \rho\rho_f^2(c_{11} + c_{33}) + \rho_f^4, \\
T_{32} &= \rho c_{33}\{c_{11}(B_5 + 2B_1 + B_2) - \rho B_8 - 2\rho_f B_6\} + \rho_f^2\{\rho B_8 + 2\rho_f B_6 + c_{11}(2B_1 + B_2) + c_{33}B_5\}, \\
T_{33} &= c_{33}\rho B_8(B_5 + 2B_1 + B_2) + c_{11}c_{33}B_5(2B_1 + B_2) + \rho_f^2\{B_6^2 - B_8(2B_1 + B_2)\} \\
&\quad + c_{33}B_6(2\rho_f B_5 - \rho B_8),
\end{aligned}$$

$$T_{34} = c_{33}B_5\{B_6^2 - B_8(2B_1 + B_2)\}, \qquad c_{11} = c_1\rho_f/\beta' - \mathrm{i}Fb_1/\omega,$$
$$c_{33} = c_3\rho_f/\beta' - \mathrm{i}Fb_3/\omega. \tag{8}$$

The roots of equation (7) are, in general, complex. We denote these roots by $q(n)$, $n = 1, 2, \ldots, 6$. Three roots with positive real parts will correspond to the waves travelling in positive z direction and the other three roots with negative real part will correspond to the waves travelling in negative z direction. We order the six roots $q(n)$, $n = 1, 2, \ldots, 6$ such that $q(1)$, $q(2)$, $q(3)$ correspond to upgoing waves, i.e., along negative z direction and $q(6)$, $q(5)$, $q(4)$ correspond to downgoing waves, i.e., along positive z direction. These are quasi-P_f, quasi-P_s and quasi-SV waves respectively. Corresponding to these values of $q(n)$, $n = 1, 2, \ldots, 6$, the wave amplitudes a_1, a_3, b_1 and b_3 can be obtained. We denote the corresponding eigen vectors by $a_1(n)$, $a_3(n)$, $b_1(n)$ and $b_3(n)$, $n = 1, 2, \ldots, 6$. These are given by

$$a_1(n) = X_1(n)/X(n), \qquad a_2(n) = X_2(n)/X(n),$$
$$b_1(n) = X_3(n)/X(n), \qquad b_3(n) = X_4(n)/X(n),$$

where

$$\begin{aligned}
X_1(n) &= q^4(n)c_{11}(B_4B_8 - B_7^2) \\
&\quad + q^2(n)\{B_8(B_5c_{11} + B_4c_{33})/c^2 - c_{11}B_8\rho - 2c_{11}\rho_fB_7 + c_{33}(c_{11}B_4 - B_7^2/c_{33})\} \\
&\quad + \{c_{33}B_8/c^2(B_5/c^2 - \rho) - c_{11}c_{33}(B_5/c^2 - \rho) + \rho_f^2(B_8/c^2 + c_{11})\}, \\
X_2(n) &= q^3(n)c_{11}/c(B_6B_7 - B_3B_8 - B_5B_8) + q(n)/c\{[B_7(\rho_f + B_6/c^2) \\
&\quad - B_8(B_3 + B_5)/c^2]c_{33} + c_{11}\rho_fB_6 + \rho_f^2B_8 + c_{33}c_{11}(B_3 + B_5)\}, \\
X_3(n) &= q^4(n)\rho_f(B_7^2 - B_4B_8) + q^2(n)\{c_{33}B_4(\rho_f + B_6/c^2) - (c_{33}B_7 + \rho_fB_8)(B_3 + B_5)/c^2 \\
&\quad + \rho_fB_8(\rho - B_5/c^2) + \rho_fB_7(\rho_f + B_6/c^2) + \rho_fB_7^2\} + (\rho_f + B_6/c^2)\{\rho_f^2 - c_{33}(\rho - B_5/c^2)\}, \\
X_4(n) &= q^3(n)/c\{c_{11}(B_4B_6 - B_3B_7 - B_5B_7) + (B_4B_8 - B_7^2)\rho_f\} + q(n)/c\{-c_{11}\rho_f(B_3 + B_5) \\
&\quad - c_{11}(\rho - B_5/c^2)\}B_6 + \rho_fB_8(B_3 + 2B_5)/c^2 - \rho\rho_fB_8 - \rho_fB_7(\rho_f + B_6/c^2),
\end{aligned}$$

and

$$X(n) = \sqrt{[\{X_1(n)\}^2 + \{X_2(n)\}^2 + \{X_3(n)\}^2 + \{X_4(n)\}^2]}. \tag{9}$$

The displacement components can be written as

$$\begin{aligned}
u_x &= \sum_{n=1}^{6} f_n a_1(n) \exp[\mathrm{i}\omega(t - x/c - q(n)z], \\
u_z &= \sum_{n=1}^{6} f_n a_3(n) \exp[\mathrm{i}\omega(t - x/c - q(n)z], \\
U_x &= \sum_{n=1}^{6} f_n b_1(n) \exp[\mathrm{i}\omega(t - x/c - q(n)z], \\
U_z &= \sum_{n=1}^{6} f_n b_3(n) \exp[\mathrm{i}\omega(t - x/c - q(n)z],
\end{aligned} \tag{10}$$

where f_n are relative excitation factors.

3. FORMULATION OF THE PROBLEMS AND THEORY OF TRANSFER MATRIX

Case 1. We consider a transversely isotropic porous layer of thickness L overlying an elastic solid half-space and underlying a fluid half-space, as shown in Figure 1. A wave in the fluid half-space making an angle of incidence θ at the face $z = 0$ will transmit quasi P_f, quasi-P_s and quasi-SV waves in the layer. These three waves are reflected back by the face $z = L$ of the layer. In addition to these waves, two types of waves (P and SV) will be transmitted to the elastic half-space.

Let $\mathbf{V}(z)$ be the column vector made up of three components (u_x, u_z, W_z) and the three components $(\tau_{zz}, \tau_{xz}, p_f)$ in the layer, $\mathbf{A}$ be the 6×1 column vector containing amplitudes of six waves propagating in the layer:

$$\mathbf{V}(z) = [u_x, u_z, W_z, \tau_{zz}, \tau_{zx}, p_f]^{\mathrm{T}},$$
$$\mathbf{A} = [(f_1 + f_6), (f_1 - f_6), (f_2 + f_5), (f_2 - f_5), (f_3 + f_4), (f_3 - f_4)]^{\mathrm{T}}.$$

The vector $\mathbf{V}(z)$ can be expressed as the function of $\mathbf{A}$ using the following equation:

$$\mathbf{V}(z) = [\Gamma(z)]\mathbf{A}, \tag{11}$$

where $[\Gamma(z)]$ is a 6×6 matrix.

At $z = L$, $\mathbf{V}(L) = [\Gamma(L)]\mathbf{A}$ and at $z = 0$, $\mathbf{V}(0) = [\Gamma(0)]\mathbf{A}$. Therefore,

$$\mathbf{V}(0) = [\Gamma(0)][\Gamma(L)]^{-1}\mathbf{V}(L),$$

or

$$\mathbf{V}(0) = [T]\mathbf{V}(L), \tag{12}$$

where $[T] = [\Gamma(0)][\Gamma(L)]^{-1}$ is called transfer matrix which enables us to relate the displacement–stress field vector at $z = 0$, with that at the face $z = L$. The entries of $[T]$ are given in Appendix A. The inverse of the matrix $[\Gamma(L)]$ is obtained by partition method [21] in order to get the matrix $[T]$.

In the fluid, the acoustic field is described by the vector

$$\mathbf{V} = [p, v]^{\mathrm{T}}, \tag{13}$$

where p and v are the pressure and normal component of velocity in fluid. The surface impedance Z is the transfer function between pressure and velocity in fluid and it is defined as a ratio of pressure to particle velocity, i.e.,

$$Z = p/v, \tag{14}$$

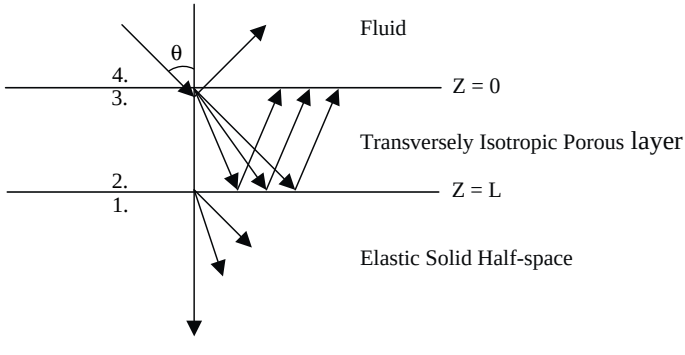

Figure 1. A transversely isotropic porous layer overlying the solid bedrock.

i.e., for a given applied pressure, the particle velocity is inversely proportional to the surface impedance.

In elastic half-space, the expressions for potential can be written as

$$\phi = \phi' \exp(-igz), \qquad \psi = \psi' \exp(-ihz).$$

Here, the factor $\exp\{i(\omega t - \sigma x)\}$ is omitted for the sake of brevity and $\sigma = k \sin\theta$,

$$g = (\omega^2/\alpha^2 - \sigma^2)^{1/2}, \qquad h = (\omega^2/\beta^2 - \sigma^2)^{1/2},$$

α and β are the velocities of P and SV waves respectively.

The displacement-stress field in the elastic solid half-space is described by vector

$$\mathbf{W_1} = [u_x, u_z, \tau_{zz}, \tau_{zx}]^{\mathrm{T}}. \tag{15}$$

The vector $\mathbf{W_1}$ can be written as

$$\mathbf{W}_1 = [\varepsilon] \begin{bmatrix} \phi' \\ \psi' \end{bmatrix}, \tag{16}$$

where $[\varepsilon]$ is a 4×2 matrix.

4. BOUNDARY CONDITIONS AND SURFACE IMPEDANCE

The interface between porous layer and elastic half-space is considered to be an imperfect interface, therefore, the boundary conditions at such interface were defined by Vashisth *et al.* [16] and these are

$$\begin{aligned} &u_{z2} = u_{z1}, \qquad W_{z2} = 0, \qquad \tau_{zz2} = \tau_{zz1}, \\ &\tau_{zx2} = \tau_{zx1}, \qquad \psi(u_{x1} - u_{x2})\mu/\beta = (1 - \psi)\tau_{zx1}, \end{aligned} \tag{17}$$

where ψ is the bonding parameter. The value of ψ is one for the case of welded contact and zero for smooth contact. The intermediate values of ψ correspond to the loose contact. β is the shear wave velocity in elastic solid half-space. Subscripts 1 and 2 correspond to the values obtained at the interface between solid half-space and porous layer, respectively, as shown in Figure 1.

The boundary conditions at the interface between fluid and porous layer are

$$(1 - \beta')u_{z3} + \beta' W_{z3} = u_4, \quad \tau_{zz3} = -(1 - \beta')p_4, \tag{18, 19}$$

$$p_{f3} = -\beta' p_4, \quad \tau_{zx3} = 0. \tag{20, 21}$$

Subscripts 3 and 4 represent the values of quantities in the porous layer and fluid half-space respectively, at the interface.

An interfacial matrix $[\eta]_{6\times4}$ relating $\mathbf{V_2}$ to $\mathbf{W_1}$ is obtained from the boundary conditions (17)–(21) and we write $\mathbf{V_2} = [\eta]\mathbf{W_1}$.

Therefore,

$$\mathbf{V}_3 = [T][\eta][\varepsilon] \begin{bmatrix} \phi' \\ \psi' \end{bmatrix} \quad \text{or} \quad \mathbf{V}_3 = [\xi] \begin{bmatrix} \phi' \\ \psi' \end{bmatrix},$$

where

$$[\xi] = [T][\eta][\varepsilon]. \tag{22}$$

and is given in Appendix B.

Using equation (22), equations (18)–(20) can be expressed in the form of ϕ' and ψ' as

$$[(1-\beta')\xi_{21}+\beta'\xi_{31}]\phi'+[\xi_{22}(1-\beta')+\beta'\xi_{32}]\psi'=p_4/\mathrm{i}\omega Z, \tag{23}$$

$$\xi_{41}\phi'+\xi_{42}\psi'=-(1-\beta')p_4, \quad \xi_{61}\phi'+\xi_{62}\psi'=-\beta' p_4. \tag{24, 25}$$

For the non-trivial solution, the determinant of the coefficients ϕ' and ψ' must vanish which gives the expression for impedance as

$$Z=(\xi_{41}\xi_{62}-\xi_{42}\xi_{61})/\{[\xi_{22}(1-\beta')+\beta'\xi_{32}][-\xi_{41}\beta'+(1-\beta')\xi_{61}] - [\xi_{21}(1-\beta')+\beta'\xi_{31}][\xi_{42}\beta'-(1-\beta')\xi_{62}]\}\mathrm{i}\omega. \tag{26}$$

This expression of impedance has been obtained by using the technique of transfer matrix. The transfer matrix method is used to transfer the boundary conditions from outer surface of the layered medium to the other via matrix multiplication. In other techniques, computation of surface impedance for the considered model involves the expansion of a determinant of order nine and that too over complex field. Thus the codes used for numerical computation of surface impedance from expression (26) are certainly efficient than those without using matrix method.

Case 2. Now we consider a two-layered transversely isotropic porous medium, backed by a rigid floor. The top layer is in contact with fluid half-space, as shown in Figure 2. Let β_{I} and β_{II} are the porosities of two layers respectively. A plane wave is incident from fluid on face A of the medium.

The presence of rigid surface at the back of the layered medium requires that normal component of fluid velocity and z- and x-components of frame velocity must vanish at surface C. The boundary conditions at the fluid–porous layer interface are same as specified in equations (17). The global transfer matrix for this layered medium will be $[T]=[T_{\mathrm{I}}][T_t][T_{\mathrm{II}}]$, where $[T_{\mathrm{I}}]$ and $[T_{\mathrm{II}}]$ are transfer matrices for layers I and II, respectively, and $[T_t]$ is the transition matrix and is obtained by the continuity of displacement–stress field vector at interface B. The expression for the surface impedance (Z) can be obtained by repeating the same steps as in case 1 and is given by

$$Z=(\Delta_5\Delta_8-\Delta_6\Delta_7)/[(1-\beta_{\mathrm{I}})^2(\Delta_2\Delta_7-\Delta_1\Delta_8)+\beta_{\mathrm{I}}(1-\beta_{\mathrm{I}})(\Delta_6\Delta_1-\Delta_2\Delta_5 - \Delta_3\Delta_8+\Delta_4\Delta_7)+\beta_{\mathrm{I}}^2(\Delta_3\Delta_6-\Delta_4\Delta_5)],$$

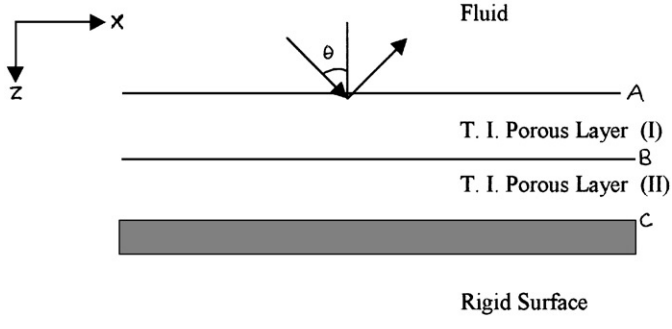

Figure 2. A two-layered transversely isotropic medium backed by a rigid floor.

where

$$\Delta_1 = t_{24}t_{55} - t_{25}t_{54}, \quad \Delta_2 = t_{26}t_{55} - t_{25}t_{56}, \quad \Delta_3 = t_{34}t_{55} - t_{35}t_{54},$$
$$\Delta_4 = t_{36}t_{55} - t_{35}t_{56}, \quad \Delta_5 = t_{44}t_{55} - t_{45}t_{54}, \quad \Delta_6 = t_{46}t_{55} - t_{45}t_{56},$$
$$\Delta_7 = t_{64}t_{55} - t_{65}t_{54}, \quad \Delta_8 = t_{66}t_{55} - t_{65}t_{56},$$

t_{ij} are the elements of global transfer matrix $[T]$.

5. NUMERICAL RESULTS AND DISCUSSION

Numerical calculations are done for the above-mentioned two cases, one for low-frequency and other in high-frequency range.

5.1. SEDIMENTARY LAYER BETWEEN WATER AND ELASTIC BEDROCK

This model finds its application in seismological studies. The sedimentary layer of the bottom is modelled as anisotropic porous layer. A contrast in the acoustic impedance gives rise to seismic reflection. Therefore the study is used to identify mismatches at the interface. The primary object of this paper has been to study the reflection of energy through ocean bottoms. Reflection coefficient can be expressed in a very simple way through impedance of media. The use of impedance simplifies the boundary conditions and makes it much easier to obtain solutions of all kinds of boundary-value problems including the reflection of plane waves. The two boundary conditions can be replaced by the single condition, i.e.,

$$Z = p/v. \tag{27}$$

The upper fluid half-space is considered as water and the underlying sedimentary layer is portrayed as transversely isotropic porous solid layer. The lower half-space is considered to represent elastic bedrock of the sediments under ocean. The values of physical properties of the sediments, used to calculate the surface impedance, are taken from Yammamato [22]. These are (in C.G.S. units)

$K_s = (5{\cdot}33 \times 10^{11},\ 15{\cdot}99 \times 10^{9})$
$E_s = (5{\cdot}332 \times 10^{11},\ 10{\cdot}64 \times 10^{8})$
$\rho_s = 2{\cdot}65$
$K_f = 2{\cdot}3 \times 10^{10}$
$\xi = 1{\cdot}0 \times 10^{-4}$
$\mu_s = (2{\cdot}0 \times 10^{11},\ 4{\cdot}0 \times 10^{9})$
$v_s = 0{\cdot}33$
$\rho_f = 1{\cdot}025$
$\beta' = 0{\cdot}30$
$\xi = 1{\cdot}0 \times 10^{-4}$

In elastic half-space

$$\lambda = 2{\cdot}5 \times 10^{11}, \qquad \mu = 3{\cdot}7 \times 10^{11}, \qquad \rho = 2{\cdot}6.$$

The constant sound speed in water is taken as 1.37×10^5 cm/s. Results for this model are computed in the low-frequency range, which is valid assumption for seismological studies.

The fluid-layered bottom interface is presenting complex impedance Z to incident wave. The real part of surface impedance represents surface resistance and imaginary part corresponds to the reactance. Figures 3(a–c) depict the magnitude of complex surface impedance at different levels of thickness of sedimentary layer as a function of the frequency. The results are in qualitative agreement with those existing in the text of seismic waves [23]. The pattern of the variation of the surface impedance with frequency is of same nature as that of amplitude spectrum mentioned in the text. The interface between sedimentary layer and elastic bedrock is considered to be imperfect and results for two

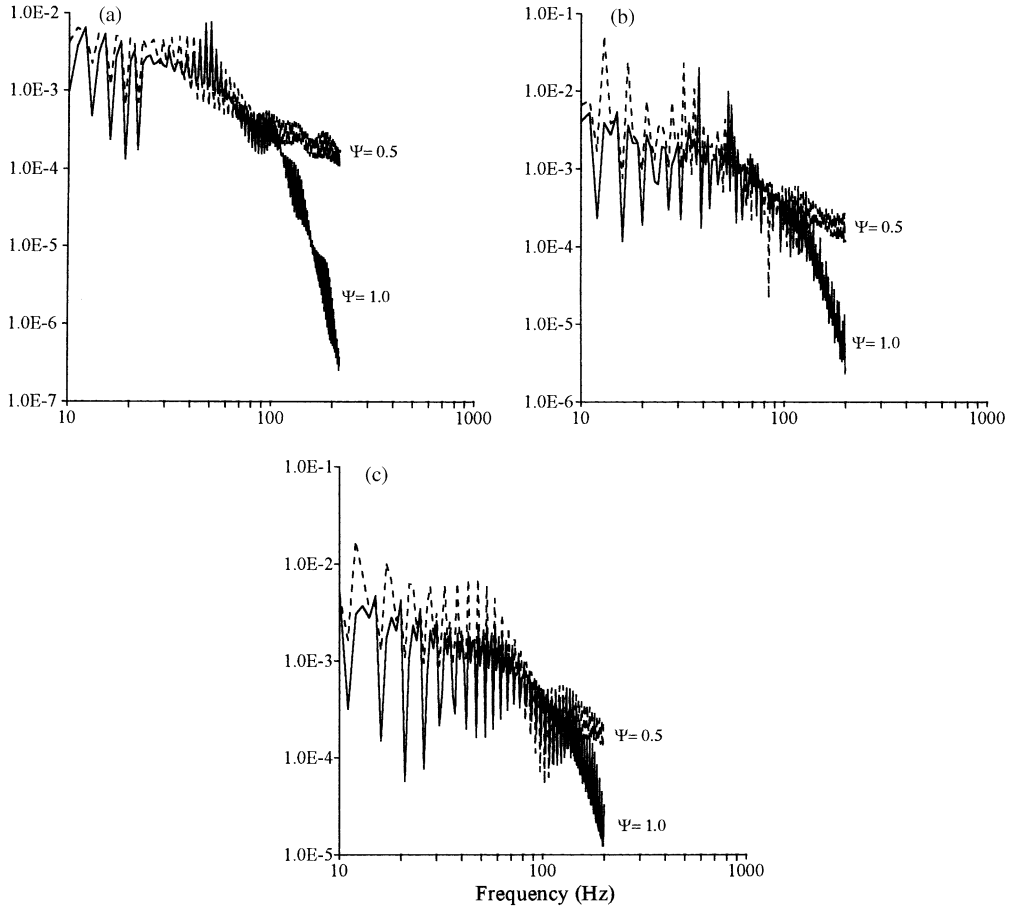

Figure 3. Surface impedance(absolute value) versus frequency at incidence angle 15° and thickness of layer: (a) 0·5 km; (b) 0·4 km; (c) 0·3 km.

particular cases are shown. The first case is the particular case when the interface between sedimentary layer and elastic solid half-space is an ideal interface ($\Psi = 1{\cdot}0$), i.e., the situation when component of tangential displacement is continuous. In the second case the results have been shown for a loosely bonded interface ($\Psi = 0{\cdot}5$). It is added that numerical calculations have been made for the other values of $\Psi(0 < \Psi < 1)$ also, which do not vary significantly from the case ($\Psi = 0{\cdot}5$) and hence are avoided to be displayed. In the frequency range of (10–100 Hz), the behavior of $|Z|$ is not much different for the perfect and imperfect boundary(see Figure 3(a)). As the frequency increases beyond 100 Hz, effect of loose boundary is felt clearly. It is noticed that the magnitude of surface impedance is more in case of loose contact than that for the case of welded contact. This behavior of Z follows that energy is being trapped at the loose boundary and hence less energy is reflected back in the medium of incidence, i.e., fluid. For relatively thin layers (Figures 3(b,c)), the magnitude of surface impedance for loosely bonded case is higher than that for perfectly bonded case in the frequency range (10–100 Hz). The reason for this may be understood from the fact that the effect of the slip at the interface is more significant when the layer's thickness is relatively small.

In the frequency range 20–100 Hz, the real part of surface impedance is noticeably different for loosely bonded and welded interface, see Figure 4(a). With the decrease of 0·1 km in the thickness of the sedimentary layer, the surface resistance changes significantly. At the frequency near 12 Hz, Re(Z) for loose contact is unusually higher in comparison to perfectly bonded case(see Figures 4(b,c)). The surface impedance is seen to be sensitive to changes in the thickness of sedimentary layer. This may be understood from the fact that the small changes in the thickness of sedimentary layer can result in a relatively large change in the gradient of the velocity profile. In particular, by changing the thickness of sedimentary layer, we are changing the wave guide-like nature of the sedimentary layer and this affects the surface impedance. As frequency increases above 100 Hz, Re(Z) becomes negligibly small which implies that in higher frequency range, it is the surface reactance which dominates and most of the energy is reflecting back. Most deep-water surfacial sea floor sediments have sound velocities less than that in overlying water. The echo sounder records very strong reflections in these areas because of sufficient impedance mismatch created at the boundary.

Figures 5(a–c) depict the magnitude of the surface impedance at a particular frequency of 20 Hz for thickness of the layer equal to 0.5, 0.4 and 0.3 km and for the whole possible

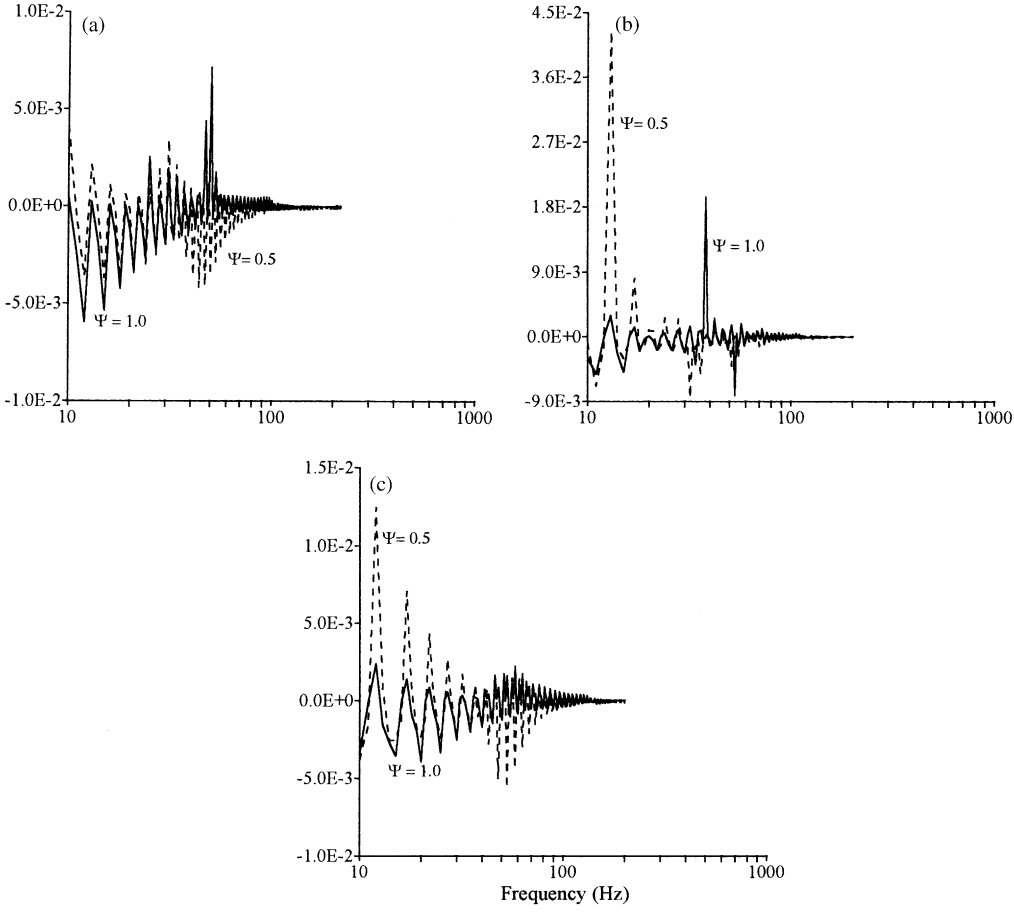

Figure 4. Surface impedance (real part) versus frequency at incidence angle 15° and thickness of layer: (a) 0·5 km; (b) 0·4 km; (c) 0·3 km.

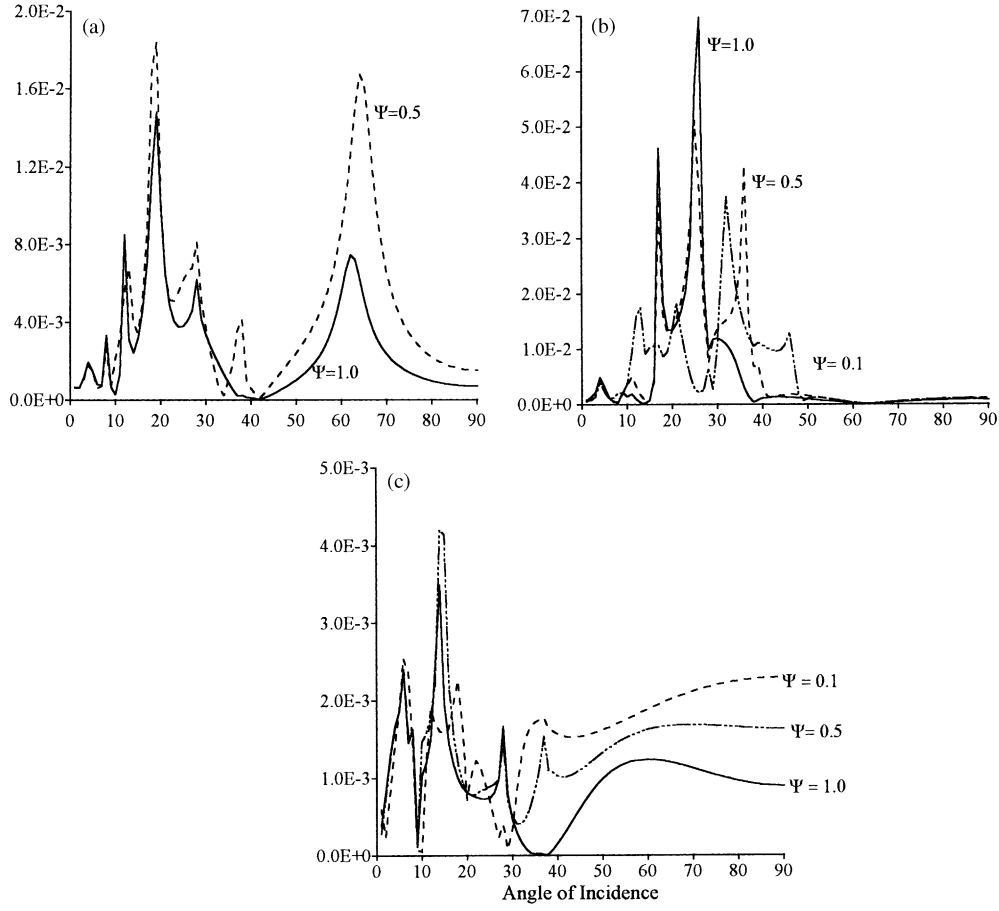

Figure 5. Surface impedance (absolute value) versus angle of incidence at frequency 20 Hz and thickness of layer: (a) 0·5 km; (b) 0·4 km; (c) 0·3 km.

range of the angle of incidence. As noted earlier, $|Z|$ in case of loosely bonded interface is greater than that in perfect bonding case. This variation is more significant near the peaks at 19° and 62° that correspond to critical angles in Figure 5(a). Angles at which the surface impedance is approaching zero correspond to the angles at which total internal reflection occurs. To study the variation of the surface impedance with the thickness of layer, the results have been calculated at three levels of thickness (0.5, 0.4 and 0.3 km). The behavior of surface impedance is considerably different with varying thickness. The position of critical angle also varies as thickness of layer is varied. The results for nearly smooth interface ($\Psi = 0{\cdot}1$) have also been computed in these cases.

In Figures 6(a–c), the variation of the real part of surface impedance is shown for three different levels of thickness. Rapid variation before the angle of incidence 30° is noticed. As the angle of incidence is increased further, Re(Z) approaches to zero. It is only the imaginary part, i.e., reactance which contributes and the boundary is said to be purely reactive. The results for nearly smooth interface ($\Psi = 0{\cdot}1$) have also been computed in these cases.

Eliminating the effect of porous layer by considering its thickness zero and neglecting the effect of elastic solid half-space, the problem reduces to the case of incidence at the free

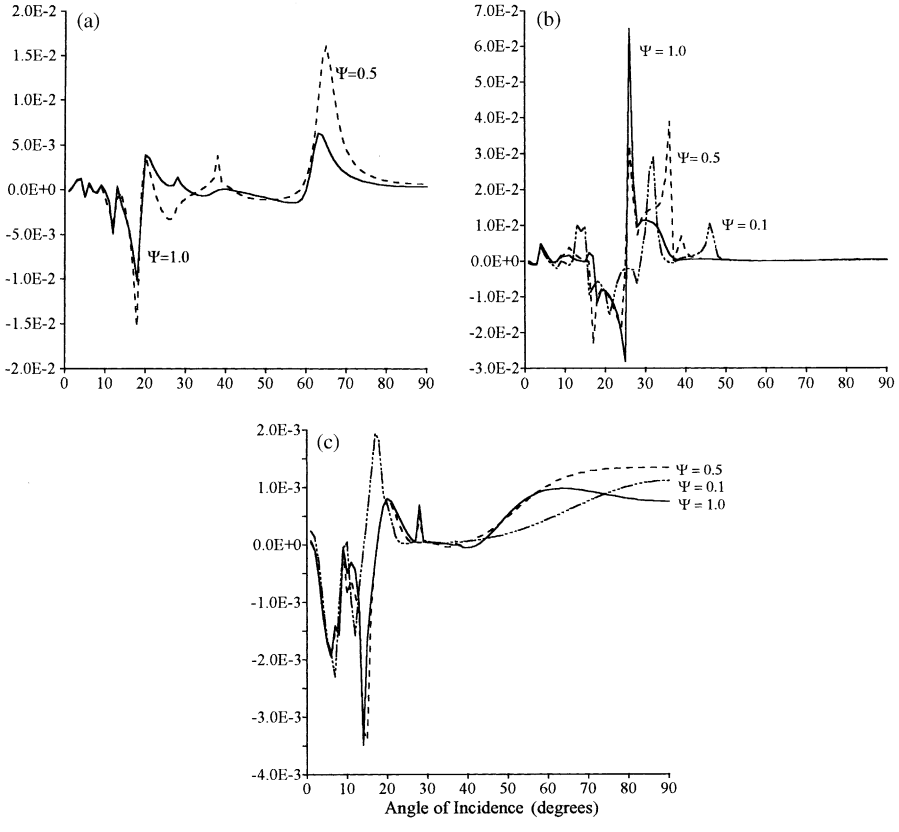

Figure 6. Surface impedance (real part) versus angle of incidence at frequency 20 Hz and thickness of layer: (a) 0·5 km; (b) 0·4 km; (c) 0·3 km.

surface of the fluid half-space. It implies automatically from equation (26) that $Z = 0$, i.e., there is no energy dissipation in this case. The whole energy that is incident on fluid half-space is reflected back in the fluid, as it should be.

5.2. A TWO-LAYERED ANISOTROPIC POROUS LAYERED MEDIUM

The model has its applications in noise control in ducts and in the study of composites. In acoustics there is a class of anisotropic media for which the boundary condition (27) is not approximate but exact. The surfaces satisfying this condition are called locally reacting surfaces. This type of surfaces is met quite frequently in architectural acoustics. Here, two layers of plastic foam are modelled as transversely isotropic porous layered medium. We adopted the values of physical parameters for the two layers of foam as given by Allard *et al.* [7] and determined the values of the material coefficients used in this paper, by using the relations mentioned therein. The values of physical parameters for transversely isotropic porous medium can be obtained from those for isotropic one by the relations

$$\frac{B_2 + 2B_1}{B_4} - 1 = 2\varepsilon, \qquad \frac{B_1}{B_5} - 1 = 2\gamma,$$

and

$$\frac{(B_3 + B_5)^2 - (B_4 - B_5)^2}{B_4(B_4 - B_5)} = 2\delta.$$

For computational purpose we take the values of ε, δ and γ as

$$\varepsilon = 0{\cdot}110, \qquad \delta = -0{\cdot}035 \quad \text{and} \quad \gamma = 0{\cdot}255.$$

Using these values of material coefficients, the surface impedance is computed in the high-frequency range. The real and imaginary parts of surface impedance are shown in Figure 7. For the verification of transfer matrix determined in this paper, justification of numerical computation and to study the effects of transversely isotropy, the calculations have been done for the case when both the porous layers are isotropic, i.e., by setting the values of ε, δ and γ to be zero. The results in this situation should be in agreement with those obtained by Allard *et al.* [7] and these are found so. The transverse isotropy of layers is found to increase both real and imaginary parts of the surface impedance. It follows that the more energy is dissipated within the anisotropic layers.

6. CONCLUSION

Wave propagation in layered porous media is studied by observing the behavior of surface impedance with frequency and angle of incidence. Detailed algebraic calculations have been made to obtain the compact analytical expressions of surface impedance at fluid–anisotropic porous layer interface in both of cases using transfer matrix. By the use of transfer matrix, we obtain a compact expression for surface impedance, which is easier to be computed numerically even when we are working in the complex field. The advantage with transfer matrix in studies of multi-layered medium is that it provides a better survey of whole expression which otherwise become very large and complicated by direct approach. The magnitude and real part of surface impedance with varying frequency and for whole range of angle of incidence is studied. This is observed that

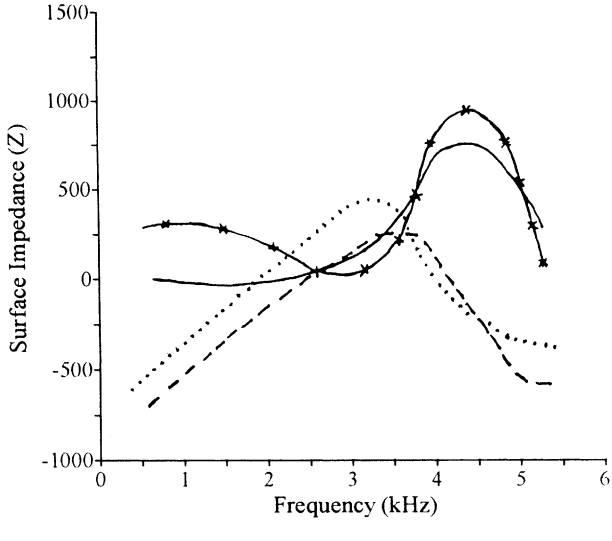

Figure 7. Surface impedance varying with frequency.

surface impedance shows the same behavior in different but small frequency pockets. The magnitude of surface impedance is sensitive to the thickness of layer.

The anisotropy of the material considered is found to affect the surface impedance. It is shown in one case that transverse isotropy increases the surface impedance.

The assumption of loosely bonded interface instead of perfect one in first case is reasonable and more realistic for layered structures having fluid-saturated porous layers. The results are calculated for different degree of bonding ranging from no bonding to full bonding between the media. Imperfectness of the interface is found to affect the reflection–transmission phenomena considerably. The results show consistency with the physical laws. The increased magnitude of surface impedance in case of imperfect interface shows that there is loss of energy due to loose bonding at the interface.

ACKNOWLEDGMENTS

The authors would like to thank the reviewers for the critical analysis and their valuable suggestions.

REFERENCES

1. M. A. Biot 1956 *Journal of the Acoustical Society of America* **28**, 168–178. Theory of propagation of elastic waves in a fluid-saturated porous solid. I: low frequency range.
2. M. A. Biot 1956 *Journal of the Acoustical Society of America* **28**, 179–191. Theory of propagation of elastic waves in a fluid saturated porous solid. II: high frequency range.
3. P. B. Nagy, L. Adler and B. P. Bonner 1990 *Applied Physics Letters* **56**, 2504–2506. Slow wave propagation in air filled porous materials and natural rocks.
4. M. J. Buckingham 1999 *Journal of the Acoustical Society of America* **106**, 575–587. Theory of compressional and transverse wave propagation in consolidated porous media.
5. M. J. Buckingham 1999 *Journal of the Acoustical Society of America* **106**, 1694–1703. On the phase speed and attenuation of unconsolidated marine sediments.
6. J. F. Allard, P. Bourdier and C. Depollier 1986 *Journal of Applied Physics* **60**, 1926–1929. Biot waves in layered media.
7. J. F. Allard, R. Rebillard, C. Depollier, W. Lauriks and A. Cops 1989 *Journal of Applied Physics* **66**, 2278–2284. Inhomogeneous Biot waves in layered media.
8. W. Lauriks, J. F. Allard, C. Depollier and A. Cops 1991 *Wave Motion* **13**, 329–336. Inhomogeneous waves in layered materials including fluid solid and porous layers.
9. E. L. Adler 1990. *IEEE Transactions on Ultrasonics and Ferroelectronics Frequency Control* **UFFC-37**, 485–490. Matrix methods applied to acoustics in multilayers.
10. A. H. Nayfeh 1991 *Journal of the Acoustical Society of America* **89**, 1521–1531. The general problem of elastic wave propagation in multi-layered anisotropic media.
11. A. H. Nayfeh and T. W. Taylor 1988 *Journal of the Acoustical Society of America* **84**, 2187–2191. Surface wave characteristics of fluid-loaded multi-layered media.
12. M. Badiely, L. Jaya and A. H.-D. Cheng 1994 *Journal of Computational Acoustics* **2**, 11–27. Propagator matrix for plane wave reflection from inhomogeneous anisotropic poroelastic seafloor.
13. C. Potel, de Belleval and Jean F., 1993 *Journal of the Acoustical Society of America* **93**, 2669–2677. Propagation in an anisotropic periodically multi-layered medium.
14. M. D. Sharma and M. L. Gogna 1991 *Journal of the Acoustical Society of America* **90**, 1068–1073. Wave propagation in anisotropic liquid-saturated porous solid.
15. D. P. Schmitt 1989 *Journal of the Acoustical Society of America* **86**, 2398–2421. Acoustic multiple logging transversely isotropic poro-elastic formations.
16. A. K. Vashishth, M. D. Sharma and M. L. Gogna 1991 *Geophysical Journal International* **105**, 601–617. Reflection and transmission of elastic waves at a loosely bonded interface between an elastic solid and liquid- saturated porous solid.
17. H. S. Bryan and J. S. Bolton 2000 *Journal of the Acoustical Society of America* **107**, 1131–1152. A transfer matrix approach for estimating the characteristic impedance and wave number of limp and rigid porous materials.

18. M. A. Biot 1962 *Journal of Applied Physics* **33**, 1482–1498. Mechanics of deformation and acoustic propagation in porous media.
19. Z. Hashin and B. W. Rosen 1964 *Journal of Applied Mechanics* **31**, 223–232. The elastic moduli and fiber reinforced materials.
20. R. M. Christensen 1979 *Mechanics of Composite Materials*. NewYork: Wiley.
21. G. Hadley, *Linear Algebra*, pp. 107–109. Narosa Publishing Company.
22. T. Yammamato 1983 *Journal of the Acoustical Society of America* **83**, 1587–1596. Acoustic propagation in the ocean with a poro elastic bottom.
23. L. Thorne and T. C. Wallace, *Modern Global Seismology*. p. 375. New York: Academic Press.

APPENDIX A

$$t_{11} = [a_1(1)\cos\theta_1 - Ha_1(2)\cos\theta_2 + H^* a_1(3)\cos\theta_3]/M,$$

$$t_{21} = \mathrm{i}[a_3(1)\sin\theta_1 - Ha_3(2)\sin\theta_2 + H^* a_3(3)\sin\theta_3]/M,$$

$$t_{31} = \mathrm{i}[b_3(1)\sin\theta_1 - Hb_3(2)\sin\theta_2 + H^* b_3(3)\sin\theta_3]/M,$$

$$t_{41} = [-C_1\cos\theta_1 + HC_2\,cos\,\theta_2 - H^* C_3\cos\theta_3]/M,$$

$$t_{51} = \mathrm{i}[-D_1\sin\theta_1 + HD_2\sin\theta_2 - H^* D_3\sin\theta_3]/M,$$

$$t_{61} = [-P_1\cos\theta_1 + HP_2\cos\theta_2 - H^* P_3\cos\theta_3]/M,$$

$$t_{12} = \mathrm{i}[a_1(1)\sin\theta_1 - Ga_1(2)\sin\theta_2 + G^* a_1(3)\sin\theta_3]/N,$$

$$t_{22} = [a_3(1)\cos\theta_1 - Ga_3(2)\cos\theta_2 + G^* a_3(3)\cos\theta_3]/N,$$

$$t_{32} = [b_3(1)\cos\theta_1 - Gb_3(2)\cos\theta_2 + G^* b_3(3)\cos\theta_3]/N,$$

$$t_{42} = \mathrm{i}[-C_1\,sin\,\theta_1 + GC_2\sin\theta_2 - G^* C_3\sin\theta_3]/N,$$

$$t_{52} = [-D_1\cos\theta_1 + GD_2\cos\theta_2 - G^* D_3\cos\theta_3]/N,$$

$$t_{62} = \mathrm{i}[-P_1\sin\theta_1 + GP_2\sin\theta_2 - G^* P_3\sin\theta_3]/N,$$

$$t_{13} = \mathrm{i}[-a_1(1)\sin\theta_1 Q_1/N + a_1(2)\sin\theta_2 Q_2 - a_1(3)\sin\theta_3 Q_3],$$

$$t_{23} = [-a_3(1)\cos\theta_1 Q_1/N + a_3(2)\cos\theta_2 Q_2 - a_3(3)\cos\theta_3 Q_3],$$

$$t_{33} = [-b_3(1)\cos\theta_1 Q_1/N + b_3(2)\cos\theta_2 Q_2 - b_3(3)\cos\theta_3 Q_3],$$

$$t_{43} = \mathrm{i}[C_1\sin\theta_1 Q_1/N - C_2\sin\theta_2 Q_2 + C_3\sin\theta_3 Q_3],$$

$$t_{53} = [D_1\cos\theta_1 Q_1/N - D_2\cos\theta_2 Q_2 + D_1\cos\theta_3 Q_3],$$

$$t_{63} = \mathrm{i}[P_1\sin\theta_1 Q_1/N - P_2\sin\theta_2 Q_2 + P_3\sin\theta_3 Q_3],$$

$$t_{14} = [-a_1(1)\cos\theta_1 R_1/M - a_1(2)\cos\theta_2 R_2 + a_1(3)\cos\theta_3 R_3],$$

$$t_{24} = \mathrm{i}[-a_3(1)\sin\theta_1 R_1/M - a_3(2)\sin\theta_2 R_2 + a_3(3)\cos\theta_3 R_3],$$

$$t_{34} = [-b_3(1)\sin\theta_1 R_1/M - b_3(2)\sin\theta_2 R_2 + b_3(3)\sin\theta_3 R_3],$$

$$t_{44} = [C_1 \cos\theta_1 R_1/M + C_2 \cos\theta_2 R_2 - C_3 \cos\theta_3 R_3],$$

$$t_{54} = \mathrm{i}[D_1 \sin\theta_1 R_1/M + D_2 \sin\theta_2 R_2 - D_3 \sin\theta_3 R_3],$$

$$t_{64} = [P_1 \cos\theta_1 R_1/M + P_2 \cos\theta_2 R_2 - P_3 \cos\theta_3 R_3],$$

$$t_{15} = \mathrm{i}[-a_1(1)\sin\theta_1 S_1/N + a_1(2)\sin\theta_2 S_2 - a_1(3)\sin\theta_3 S_3],$$

$$t_{25} = [-a_3(1)\cos\theta_1 S_1/N + a_3(2)\cos\theta_2 S_2 - a_3(3)\cos\theta_3 S_3],$$

$$t_{35} = [-b_3(1)\cos\theta_1 S_1/N + b_3(2)\cos\theta_2 S_2 - b_3(3)\cos\theta_3 S_3],$$

$$t_{45} = \mathrm{i}[C_1 \sin\theta_1 S_1/N - C_2 \mathit{sin}\,\theta_2 S_2 + C_3 \sin\theta_3 S_3],$$

$$t_{55} = [D_1 \cos\theta_1 S_1/N - D_2 \cos\theta_2 S_2 + D_3 \cos\theta_3 S_3],$$

$$t_{65} = \mathrm{i}[P_1 \sin\theta_1 S_1/N - P_2 \sin\theta_2 S_2 + P_3 \sin\theta_3 S_3],$$

$$t_{16} = [-a_1(1)\cos\theta_1 L_1/M + a_1(2)\cos\theta_2 L_2 - a_1(3)\cos\theta_3 L_3],$$

$$t_{26} = \mathrm{i}[-a_3(1)\sin\theta_1 L_1/M + a_3(2)\sin\theta_2 L_2 - a_3(3)\sin\theta_3 L_3],$$

$$t_{36} = \mathrm{i}[-b_3(1)\sin\theta_1 L_1/M + b_3(2)\sin\theta_2 L_2 - a_3(3)\sin\theta_3 L_3],$$

$$t_{46} = [C_1 \cos\theta_1 L_1/M - C_2 \cos\theta_2 L_2 + C_3 \cos\theta_3 L_3],$$

$$t_{56} = \mathrm{i}[D_1 \sin\theta_1 L_1/M - D_2 \sin\theta_2 L_2 + D_3 \sin\theta_3 L_3],$$

$$t_{66} = [P_1 \cos\theta_1 L_1/M - P_2 \cos\theta_2 L_2 + P_3 \cos\theta_3 L_3]$$

where

$$X = [D_3 b_3(2) - D_2 b_3(3)]/D_3, \qquad Y = [C_3 P_2 - C_2 P_3]/P_3,$$
$$M = a_1(1) + C_1 R_1 + P_1 L_1,$$
$$Q_2 = [1/X + GQ_1/N], \qquad N = a_3(1) - b_3(1)Q_1 - D_1 S_1,$$
$$G = [b_3(1)D_3 - b_3(3)D_1]/XD_3,$$
$$H = [P_3 C_1 - C_3 P_1]/YP_3, \qquad H^* = [P_2 C_1 - C_2 P_1]/YP_3,$$
$$Q_3 = [D_2/XD_3 + G^* Q_1/N],$$
$$G^* = [b_3(1)D_2 - b_3(2)D_1]/XD_3, \qquad S_2 = [b_3(3)/XD_3 + GS_1/N],$$
$$L_2 = [C_3/YP_3 + HL_1/M],$$
$$L_1 = [a_1(2)C_3 - a_1(3)C_2]/YP_3, \qquad R_1 = [-P_3 a_1(2) + P_2 a_1(3)]/YP_3,$$
$$R_2 = [1/Y - HR_1/M],$$
$$Q_1 = [D_3 a_3(2) - a_3(3)D_2]/XD_3, \qquad S_1 = [a_3(2)b_3(3) - a_3(3)b_3(2)]/XD_3,$$
$$R_3 = [P_2/YP_3 - H^* R_1/M], \qquad L_3 = [C_2/YP_3 + H^* L_1/M],$$
$$S_3 = [b_3(2)/XD_3 + G^* S_1/N], \qquad C_j = \mathrm{i}[B_4 \lambda j a_3(j) + a_3(j)B_3 + b_1(j)B_7 + b_3(j)B_7 \lambda j],$$
$$D_j = \mathrm{i}[B_4 \lambda_j a_1(j) + a_3(j)B_5],$$
$$P_j = \mathrm{i}[B_3 a_1(j) + a_3(j)B_7 \lambda j + b_1(j)B_8 + b_3(j)B_8 \lambda j],$$
$$\lambda j = cq(j), \qquad \theta_j = \omega q(j)L, \quad \omega \text{ the frequency of incident wave } (j = 1, 3),$$

APPENDIX B

$$\xi_{j1} = -\mathrm{i}\sigma x_j - \mathrm{i}g y_j + [\lambda(g^2+\sigma^2) - 2\mu g^2] z_j + 2\mu\sigma g p_j, \quad j = (1,2,\ldots,6)$$
$$\xi_{j2} = \mathrm{i}h x_j - \mathrm{i}\sigma y_j - 2\mu\sigma h z_j - \mu(\sigma^2 - h^2) p_j,$$

where

$$x_j = t_{j1} + (t_{j4} - t_{j6}) t_{51}/(t_{56} - t_{54}),$$
$$y_j = (t_{j2} + t_{j3}) + (t_{j4} - t_{j6})(t_{52} + t_{53})/(t_{56} - t_{54}),$$
$$z_j = (t_{j4} t_{56} - t_{j6} t_{54})/(t_{56} - t_{54}),$$
$$p_j = (t_{j4} - t_{j6}) t_{55}/(t_{56} - t_{54}) + t_{j1}\mathrm{i}(1-\psi)\beta/(\omega\mu\psi) + t_{j5}.$$